THE JOURNAL OF PHYSICAL CHEMISTRY B LETTERS

2005, *109,* 6963−6967
Published on Web 03/25/2005

Preferential Growth of Single-Walled Carbon Nanotubes on Silica Spheres by Chemical Vapor Deposition

Weiwei Zhou,[†] Yan Zhang,[†] Xuemei Li,[†] Shiling Yuan,[‡] Zhong Jin,[†] Junjian Xu,[†] and Yan Li*,[†]

Key Laboratory for the Physics and Chemistry of Nanodevices, College of Chemistry and Molecular Engineering, Peking University, Beijing 100871, China, and Key Laboratory of Colloid and Interface Chemistry, Shandong University, Jinan, Shandong 250100, China

Received: February 4, 2005; In Final Form: March 16, 2005

The preferential growth of single-walled carbon nanotubes (SWNTs) on silica spheres with various diameters was realized for the first time by chemical vapor deposition (CVD) of methane. SWNTs tend to wrap the silica spheres to form a new superstructure of uniform SWNT nanoclaws when the diameters of the silica spheres are larger than 400 nm. The SWNTs obtained on silica spheres have highly graphitic tubular walls as characterized by Raman spectroscopy and HRTEM. This is a new method to obtain tunable uniform elastic deformation of SWNTs, which may act as the model for the study about the effect of delocalized bending on the properties of SWNTs. In addition, the combination of SWNTs with monodispersed silica spheres could conveniently integrate SWNTs into photonic crystals.

I. Introduction

Carbon nanotubes (CNTs) have attracted extensive attention due to their extraordinary electrical, chemical, optical, and mechanical properties[1−3] since they were discovered by Iijima in 1991.[4] Single-walled nanotubes (SWNTs), as an atomically well-defined one-dimensional system, have been a strong focus due to their promising applications in nanometer-scaled electronic devices such as transistors,[5−7] logic gates,[8] and sensors.[9,10] Recently, significant progress has been made in controlling the growth site,[11,12] the orientation,[13−15] and the diameter of straight SWNTs[16−20] on flat silicon substrates by the CVD method. Comparing with straight SWNTs whose electrical properties are determined by the diameter and the chirality, many theoretical calculations and experiments have demonstrated that the electrical properties of the curved SWNTs are strongly influenced by the bending degree.[21−25] For example, Dai et al. detected that the electrical behavior of the curved SWNTs was related to the local defects created by bending the SWNTs using an AFM tip.[25] In the meantime, various curved structures of SWNTs such as toris and coils were obtained on the flat substrate and in bulk. Liu et al. first observed a small amount of carbon nanorings in bulk CNTs synthesized by laser ablation.[26] A similar result was also reported in CNTs produced catalytically by thermal decomposition of gaseous hydrocarbons.[27] Furthermore, Martel et al. reported that nanotube rings were fabricated from oxidated straight SWNTs with the yields of over 50% by using ultrasonic irradiation.[28,29] Though closed rings of CNTs with a narrow size distribution could be synthesized in solution by covalent ring-closure reaction,[30] the low concentration of CNTs in solution limited the amount of rings obtained, and the size of the rings could not be controlled. Until now there was still no effective method to obtain a large amount of curved SWNTs with perfect graphitic structures in a controlled way.

In this paper, we prepared an interesting new structure, nanoclaws of SWNTs, by the preferential growth of SWNTs on monodispersed silica spheres using CVD of methane. The stability of the curved superstructure is attributed to the strong van der Waals interaction between the nanotubes and the substrate, which is estimated from the results of molecular dynamics (MD) and molecular mechanics (MM) simulation. Though there were some reports of synthesis of CNTs on the curved substrates in the past years,[31−33] such curved superstructures of CNTs have not been observed before.

II. Experimental Section

Preparation of Silica Spheres with Catalysts. The uniform silica spheres of different sizes were prepared according to the Stöber method.[34] The spheres were soaked in a fresh 0.01 M $FeCl_3$ aqueous solution for 30 min to deposit the Fe(III) species (such as $Fe(OH)_3$) on the surface of spheres. Then, the silica spheres were separated by centrifuging, washed three times with deionized water, and re-dispersed in ethanol for the following usage.

Chemical Vapor Deposition. The silicon wafer was cleaned by Piranha solution (a mixture of 98% H_2SO_4 and 30% H_2O_2 with the volume ratio of 7:3) for 30 min at 90 °C to make sure that the surface of the silicon wafer is hydrophilic. 1∼2 wt % ethanol solution of silica spheres was dropped onto the silicon wafer and then dried in ambient atmosphere to form a flat layer of silica spheres. The wafer was put into a horizontal quartz tube furnace and calcined in air at 700 °C for 5 min to remove the solvent and obtain iron oxide nanoparticles on the surface

* To whom correspondence should be addressed, Tel: +86-10-62756773, E-mail: yanli@ pku.edu.cn.
[†] Peking University.
[‡] Shandong University.

10.1021/jp050629u CCC: $30.25

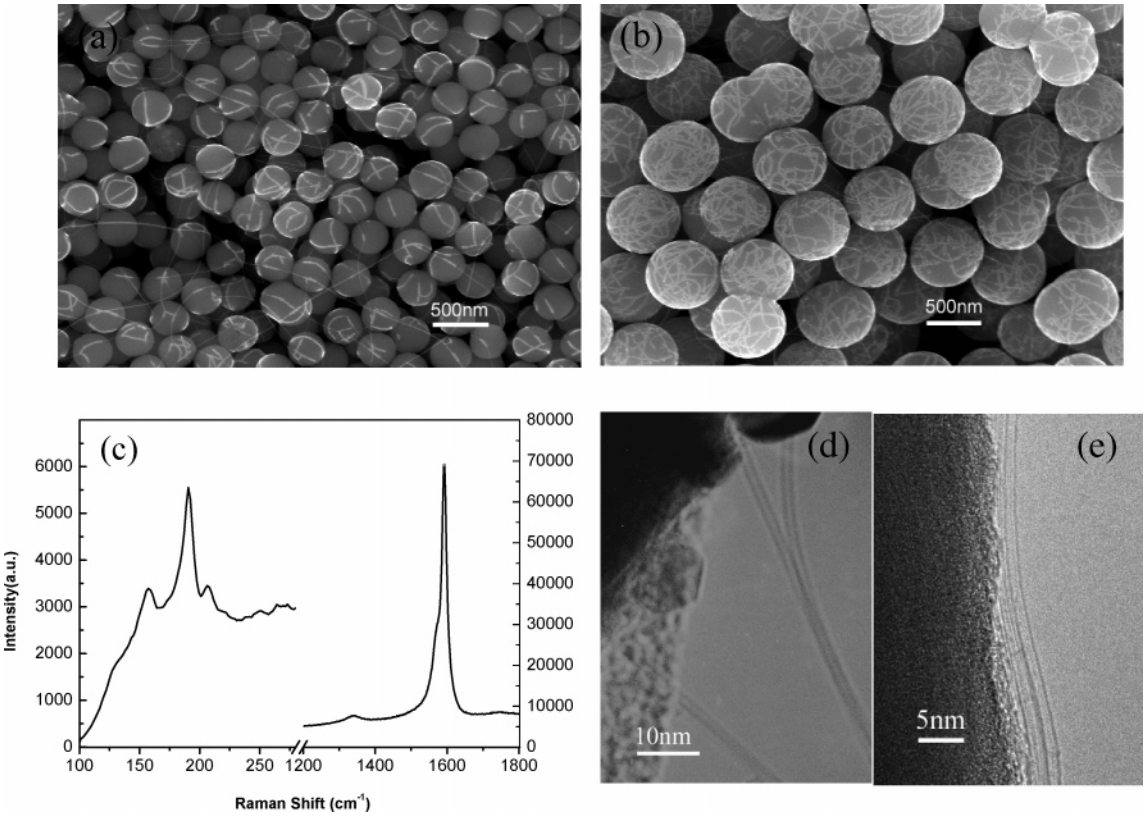

Figure 1. SEM images of SWNTs grown on silica spheres (a, 350 nm, and b, 680 nm), the corresponding Raman spectrum (c), and the HRTEM images (d and e).

of silica spheres. In a typical CVD growth experiment, the substrate was heated to 900 °C in Ar and then reduced in H_2 (220 sccm) for 5 min. Subsequently, CVD growth of SWNTs proceeded at 900 °C with CH_4 (300 sccm) as carbon source for 15 min, followed by cooling the furnace in Ar to room temperature.

Characterization. Scanning electron microscope (SEM, FEI XL30 S−FEG, the operating voltage is 10 kV), high-resolution transmission electron microscope (HRTEM, Hitachi 9000, operated at 100 kV and Tecnai F30 FEG-TEM, operated at 150 kV), and micro-Raman spectroscope (Renishaw 1000) were used to characterize the produced SWNTs. The excitation wavelength of micro-Raman is 514.5 nm sourced by an Ar ion laser. For HRTEM, the samples were scraped from silicon wafers onto the Cu grids.

III. Molecular Simulation

All molecular mechanics and dynamics calculations were performed using the program of Materials Studio 3.0. The Dynamics and Minimizer modules were used to optimize the structures and calculate the energies of different simulation systems. COMPASS force field was employed in the simulation. van der Waals and Coulomb interactions were calculated using atom-based cutoff method with a cutoff distance of 45 Å. MD simulations were carried out in the NVT (Constant- volume/ constant-temperature dynamics) ensemble with a time step of 1 fs. The dynamics was modified to allow the system to exchange heat with the environment at a controlled temperature. The Hoover−Nosé thermostat method was used to control the temperature at 300 K.

The initial configuration was prepared as follows. First, to simulate the real system, that is, the amorphous surface of a silica sphere, an amorphous silicon dioxide surface was introduced. As there are very few −OH groups on silica surfaces at high temperature,[35] we did not consider −OH groups in the calculation. It is normally accepted that there are no chemical bonds formed between carbon SWNTs and silica surfaces.[36,37] Therefore, we took only the nonbonding interactions into consideration. Since the periodic condition was used in the simulation, the silicon dioxide surface should be considered as a repeating cell at both horizontal and vertical directions. To eliminate the influence of other surfaces in the vertical direction, we enlarged the length of *Z*-axis to 240 Å. Thus, the cell we used is 28.510 Å × 28.510 Å × 240 Å. Then, to simulate the actual growth process, a (10,10) nanotube comprising 400 carbon atoms and with the length of 24.4 Å was placed onto the silicon dioxide surface perpendicularly with a distance of 3∼4 Å.

IV. Results and Discussion

Figure 1a,b shows the typical SEM images of CNTs after CVD growth. The diameters of the silica spheres are 350 and 680 nm, respectively. It is obvious that the growth modes are different. In Figure 1a, most CNTs tend to span across different silica spheres; but in Figure 1b, most CNTs strongly adhere to the surface of silica spheres and follow the curvature of the sphere to form an interesting structure of nanoclaws. It should be noticed that the edge-effect charging at the CNT−silica interface enlarges the displayed diameter of CNTs in the SEM images. Therefore, SEM images of the nanotubes across the silica spheres provide a better measure of the real diameter. The Raman spectrum in Figure 1c was taken in one scan and without any accumulation. It clearly shows a typical radial breathing mode (RBM) of SWNTs (190.6 cm^{-1}). In the high-frequency region, a sharp and intensive G band is shown at 1586.3 cm^{-1}. The D band at around 1336.7 cm^{-1} is very weak, indicating

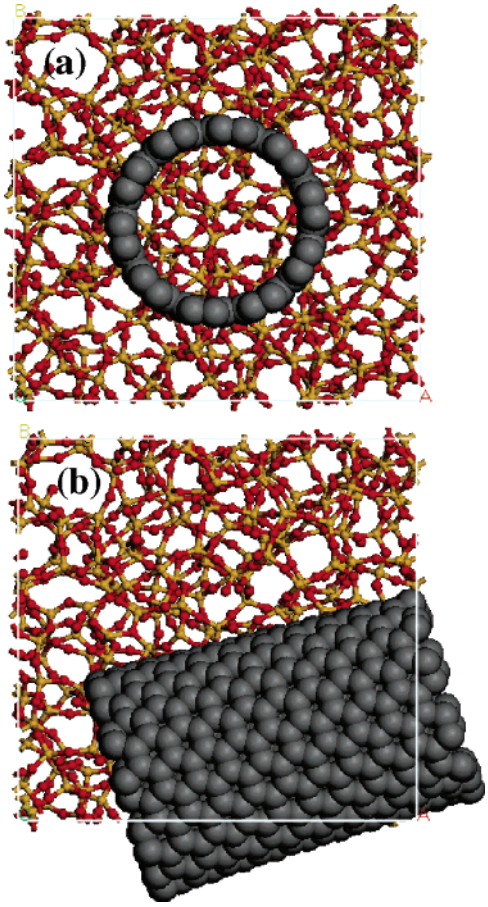

Figure 2. Initial (a) and optimized (b) geometries of a (10,10) nanotube on the silicon dioxide surface.

that the SWNTs grown on the silica surfaces are highly graphitic and with few structural defects. As we know, bending of SWNTs is usually considered to come from the topological defects such as pentagon−heptagon pairs on SWNTs. So, we expected that there would be a high intensity of D band, due to high density of defects in CNTs. However, the experimental result demonstrates that SWNTs obtained on silica spheres have good graphitic structures. HRTEM images (Figure 1d,e) further show that very little amorphous carbon materials cover the surface of SWNTs, also indicating that the as-synthesized SWNTs are of high purity. Based on the experimental results, we consider that the bending of SWNTs is caused by the uniform elastic deformation and it should belong to a delocalized bending.[38]

Formation of the curved superstructure of SWNTs can be understood on the basis of the system energy. The extremely low D band in the Raman spectrum of Figure 1c indicates no chemical bonding between SWNTs, but there is a strong van der Waals interaction between the nanotubes and the amorphous surface of the silica spheres, so the SWNTs tend to grow along the surface of the silica spheres. The result of molecular simulation qualitatively explains the process. The initial model is shown in Figure 2a. After MD and MM simulation, the initially vertical nanotube became horizontal to the silicon dioxide surface (Figure 2b). It should be pointed out that as the periodic boundary condition was adopted in our simulation, the part of the tube which is outside the shown silica surface unit is actually still on the silica surface of neighboring units. It was calculated that the van der Waals contribution to the energy decrease of tube−silica system per unit nanotube length is 1.59 $eV \cdot nm^{-1}$ after energy minimization calculation. The result is in good accord with the Clausius−Mossotti relation[39] which yields 1.4 $eV \cdot nm^{-1}$. It seems that horizontal to surface is the low-in-energy geometry for (10,10) nanotube, indicating that (10,10) nanotube is inclined to grow along the surface.

In our experiments, we noticed that the size of silica spheres could greatly influence the growth modes of SWNTs. From SEM and HRTEM images, we observed that SWNTs have two distinct growth modes spreading from or winding the surface of silica spheres. SWNTs tend to grow along the surfaces of bigger silica spheres; on the contrary, SWNTs tend to grow away from the surfaces of smaller silica spheres. To further study the mechanism of SWNTs grown on the surface of silica spheres, we varied the size of silica spheres for the CVD growth of SWNTs at the same experimental conditions. The silica spheres with the average diameters of 300, 350, 400, 500, 580, and 680 nm were used in our experiments. We did experiments repeatedly for the silica spheres of every size. The results show very good reproducibility. Figure 3 gives the typical SEM images of the different sized silica spheres after CVD processes. From Figure 3a to Figure 3c, the common case is one SWNT passing through the surfaces of several silica spheres, and the tendency of SWNTs growing in spreading mode is quite obvious. With the increase of the size of silica spheres, the percentage of SWNTs growing along on the surface increases slightly. In Figure 3d, it turns out that the winding mode becomes dominant and only a few SWNTs spread from the surface. With the further increase of the diameters, the loops of SWNTs growing along the silica spheres also increase (Figure 3e and 3f). Finally the silica spheres were wrapped by SWNTs to form nanoclaws of SWNTs.

So the growth of SWNTs on the curved surface is greatly influenced by the curvature and other chemical and physical properties of the curved surface, and the flow of CH_4. Taking these experimental factors into consideration, we propose the growth mechanism of SWNTs on the surface of silica spheres as follows. In the initial stage of the growth, SWNTs grew up perpendicularly to the surface according to the "base-growth" mechanism, but soon SWNTs lay down because of the strong van der Waals interaction between the nanotubes and the amorphous silica surface according to the result of MD simulation, so SWNTs have the tendency to wind the surfaces of silica spheres. However, bending of the nanotubes produces the elastic energy. The reduction of the size of the silica spheres results in the more significant elastic energy of the nanotube because the curvature increases, so SWNTs prefer to spread from the curved surface to decrease the system energy. The stable mode of growth is determined by the competition between the binding energy from the van der Waals interaction of the nanotubes and the amorphous silica surface and the elastic energy from the bending of nanotubes. There exists a critical diameter. When the diameter of silica spheres is larger than the critical diameter, the SWNTs prefer to the winding mode; otherwise, SWNTs prefer the spreading mode. To roughly estimate the critical diameter, we measured the average coverage of SWNTs on 100 silica spheres for every size. Because of the two-dimensional limitation of SEM images, we approximately substitute the area of equatorial circularity of silica spheres (s) for the area of curved surface of half sphere and the length of straight line of SWNTs in SEM images (l) for the length of actual curved line of SWNTs. The average coverage (α) can be defined as $\alpha = l/s$. The average coverage was plotted against the diameter of silica spheres in Figure 4. When the diameter of silica spheres is larger than 400 nm, the curve turns to a sharp rise. So we conclude that the critical diameter is around 400 nm. In our experiments, the largest diameter of silica spheres

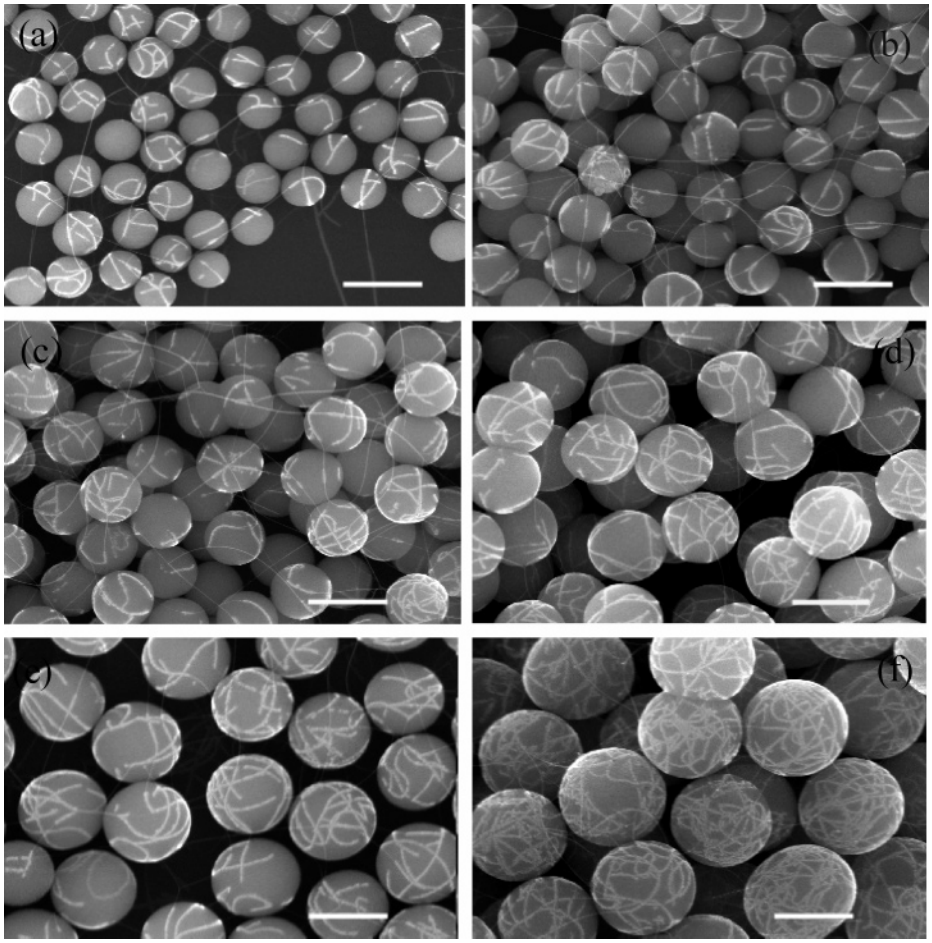

Figure 3. SEM images of SWNTs grown on silica spheres of 300, 350, 400, 500, 580, and 680 (a−f), respectively. The bar represents 500 nm.

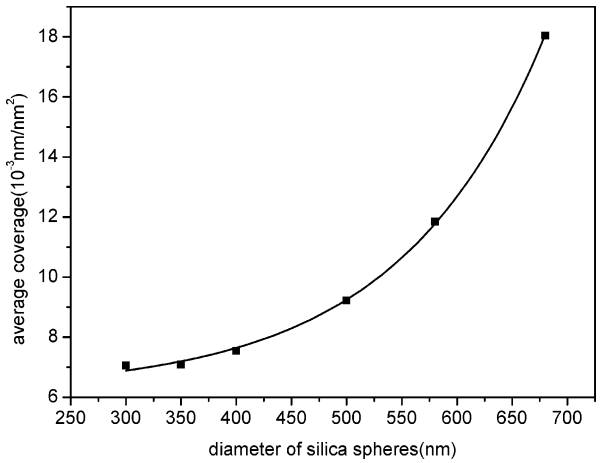

Figure 4. Relationship between the average coverage of SWNTs on silica spheres and the diameter of silica spheres.

is 680 nm. If the diameter of the silica spheres is further increased, the curvature of the spherical surface will be reduced and the growth mode of the SWNTs will be similar to that on the flat surface. Therefore, we predict that the coverage of the SWNTs on the surface will increase very slowly and finally approach a maximum.

In the above discussion, we mainly considered the thermodynamic effects. Sometimes the kinetic components may take an important role. For example, the very large flow of CH_4 can contribute to the extending of SWNTs from the substrate according to a related report,[14] However, the total flow of reaction gas is low in our experiments. We tried to interrupt the growing process by alternating the flow rate of inert gas Ar or by giving a mechanical shake to the silicon wafers during the CVD process. We found that these kinetic shocks to the system did not change the growing mode of the SWNTs. Therefore, we can conclude that the thermodynamic factors take the dominant role under our experiment conditions.

Martel et al. reported that the nanotube rings synthesized by ultrasonic irradiation have a diameter of 300−400 nm, and they attributed the formation of rings to the balance between tube−tube van der Waals adhesion and the strain energy resulting from the coiling-induced curvature.[28,29] The critical diameter that we obtained is slightly larger than theirs because it is understandable that the tube−silica van der Waals adhesion is weaker than the tube−tube adhesion. The diameters of rings synthesized by other methods are also very similar with our experimental results. For example, the average diameter of the rings was 540 nm by covalent ring-closure reaction,[30] and rings of about 500 nm in diameter and 300−500 nm in diameter were respectively observed in bulk CNTs synthesized by thermal decomposition of hydrocarbon gas[27] and laser ablation.[26]

V. Conclusion

There are two distinct growth modes of SWNTs on silica spheres: growing away from the surface or growing along the surface. The preferential growth of SWNTs on silica spheres was realized by varying the size of silica spheres. The stable mode of growth is determined by the energy competition between binding energy and elastic energy, and the critical diameter of silica spheres that the dominant growth modes of SWNTs shift is about 400 nm. The curvature of SWNTs can

be tuned by changing the size of silica spheres, and the curve caused by the elastic strain is a delocalized bending. Obviously its effects on electronic property should be largely different from that by topological defects such as pentagon−heptagon pairs. Therefore a new possibility is presented for the study of the delocalized bending of SWNTs in experiment. In addition, the nanoclaws of SWNTs also provide a convenient approach to combine CNTs with photonic crystals. An abnormally strong optical signal is observed in our Raman and fluorescence study of SWNT nanoclaws, indicating that there are some new and interesting optical properties if CNTs are confined in 3D structures. Further research on the optical properties of these nanotubes is ongoing in our lab.

Acknowledgment. This work was supported by the National Natural Science Foundation of China and The Ministry of Science and Technology of China (Project 2001CB610501).

Supporting Information Available: The discussion of the influence of the flow of CH_4 on the growth of SWNTs and Raman spectra of SWNTs on silica spheres of different size. This material is available free of charge via the Internet at http://pubs.acs.org.

References and Notes

(1) Dresselhaus, M. S., Dresselhaus, G., Avouris, Ph., Eds.; *Carbon Nanotubes Synthesis, Structures, and Applications*; Springer: Berlin, 2001.

(2) Saito, R.; Dresselhaus, M. S.; Dresselhaus, G. *Physical Propertiesof Carbon Nanotubes*; World Scientific Publishing: Singapore, 1998.

(3) Dresselhaus, M. S.; Dresselhaus, G.; Eklund, P. C. *Science of Fullerenes and Carbon Nanotubes*; Academic: New York, 1996.

(4) Iijima, S. *Nature* **1991**, *354*, 56−58.

(5) Li, S.; Yu, Z.; Yen, S.-F.; Tang, W. C.; Burke, P. J. *Nano Lett.* **2004**, *4*, 753−756.

(6) Keren, K.; Berman, R. S.; Buchstab, E.; Sivan, U.; Braun, E. *Science* **2003**, *302*, 1380−1382.

(7) Postma, H. W. Ch.; Teepen, T.; Yao, Z.; Grifoni, M.; Dekker, C. *Science* **2001**, *293*, 76−79.

(8) Derycke, V.; Martel, R.; Appenzeller, J.; Avouris, Ph. *Nano Lett.* **2001**, *1*, 453−456.

(9) Qi, P.; Vermesh, O.; Grecu, M.; Javey, A.; Wang, Q.; Dai, H.; Peng, S.; Cho, K. J. *Nano Lett.* **2003**, *3*, 347−351.

(10) Lin, Y.; Lu, F.; Tu, Y.; Ren, Z. *Nano Lett.* **2004**, *4*, 191−195.

(11) Cassell, A. M.; Franklin, N. R.; Tombler, T. W.; Chan, E. M.; Han, J.; Dai, H. *J. Am. Chem. Soc.* **1999**, *121*, 7975−7976.

(12) Jung, Y. J.; Homma, Y.; Ogino, T.; Kobayashi, Y.; Takagi, D.; Wei, B.; Vajtai, R.; Ajayan, P. M. *J. Phys. Chem. B* **2003**, *107*, 6859−6864.

(13) Su, M.; Li, Y.; Maynor, B.; Buldum, A.; Lu, J. P.; Liu, J. *J. Phys. Chem. B* **2000**, *104*, 6505−6508.

(14) Franklin, N. R.; Dai, H. *Adv. Mater.* **2000**, *12*, 890−894.

(15) Huang, S.; Cai, X.; Liu, J. *J. Am. Chem. Soc.* **2003**, *125*, 5636−5637.

(16) Cheung, C. L.; Kurtz, A.; Park, H.; Lieber, C. M. *J. Phys. Chem. B* **2002**, *106*, 2429−2433.

(17) Li, Y.; Kim, W.; Zhang, Y.; Rolandi, M.; Wang, D.; Dai, H. *J. Phys. Chem. B* **2001**, *105*, 11424−11431.

(18) Tang, Z.; Sun, H.; Wang, J.; Chen, J.; Li, G. *Appl. Phys. Lett.* **1998**, *73*, 2287−2289.

(19) An, L.; Owens, J. M.; McNeil, L. E.; Liu, J. *J. Am. Chem. Soc.* **2002**, *124*, 13688−13689.

(20) Han, S.; Yu, T.; Park, J.; Koo, B.; Joo, J.; Hyeon, T. *J. Phys. Chem. B* **2004**, *108*, 8091−8095.

(21) Han, J.; Anantram, M. P.; Jaffe, R. L.; Kong, J.; Dai, H. *Phys. Rev. B* **1998**, *57*, 14983−14989.

(22) Liu, L.; Jayanthi, C. S.; Tang, M.; Wu, S.; Tombler, T. W.; Zhou, C.; Alexseyev, L.; Kong, J.; Dai, H. *Phys. Rev. Lett.* **2000**, *84*, 4950−4953.

(23) Mazzoni, M. S. C.; Chacham, H. *Phys. Rev. B* **2000**, *61*, 7312−7315.

(24) Chibotaru, L. F.; Bovin, S. A.; Ceulemans, A. *Phys. Rev. B* **2002**, *66*, 161401.

(25) Tombler, T. W.; Zhou, C.; Alexseyev, L.; Kong, J.; Dai, H.; Liu, L.; Jayanthi, C. S.; Tang, M.; Wu, S.-Y. *Nature* **2000**, *405*, 769−772.

(26) Liu, J.; Dai, H.; Hafner, J. H.; Colbert, D. T.; Smalley, R. E.; Tans, S. J.; Dekker, C. *Nature* **1997**, *385*, 780−781.

(27) Ahlskog, M.; Seynaeve, E.; Vullers, R. J. M.; Haesendonck, C. V.; Fonseca, A.; Hernadi, K.; Nagy, J. B. *Chem. Phys. Lett.* **1999**, *300*, 202−206.

(28) Martel, R.; Shea, H. R.; Avouris, Ph. *Nature* **1999**, *398*, 299.

(29) Martel, R.; Shea, H. R.; Avouris, Ph. *J. Phys. Chem. B* **1999**, *103*, 7551−7556.

(30) Sano, M.; Kamino, A.; Okamura, J.; Shinkai, S. *Science* **2001**, *293*, 1299−1301.

(31) Huang, S. *Carbon* **2003**, *41*, 2347−2352.

(32) Lan, A.; Iqbal, Z.; Aitouchen, A.; Libera, M.; Grebel, H. *Appl. Phys. Lett.* **2002**, *81*, 433−435.

(33) Cassell, A. M.; McCool, G. C.; Ng, H. T.; Koehne, J. E.; Chen, B.; Li, J.; Han, J.; Meyyappan, M. *Appl. Phys. Lett.* **2003**, *82*, 817−819.

(34) Stöber, W.; Fink, A. *J. Colloid Interface Sci.* **1968**, *26*, 62−69.

(35) Iler, R. K. *The chemistry of silica: solubility, polymerization, colloid and surface properties, and biochemistry*; Wiley: New York, 1979.

(36) Huang, S. M.; Woodson, M.; Smalley, R.; Liu, J. *Nano Lett.* **2004**, *4*, 1024−1028.

(37) Seeger, T.; Redlich, P.; Grobert, N.; Terrones, M.; Walton, D.; Kroto, H. W.; Ruhle, M. S. *Chem. Phys. Lett.* **2001**, *339*, 41−46.

(38) Liu, L.; Jayanthi, C. S.; Wu, S. Y. *Phys. Rev. B* **2001**, *64*, 033412.

(39) Israelachvili, J. *Intermolecular and Surface Forces*; Harcourt Brace & Company: San Diego, 1997.